

VALIDATION OF THE TEMPORAL SIGNAL CHANGE CAUSED BY ACUPUNCTURE STIMULATION WITH MULTI-BAND ACQUISITION.

Tomokazu Murase¹, Masahiro Umeda², Masaki Fukunaga³, Katsuya Maruyama⁴, Yuko Kawai², Yasuharu Watanabe², Chuzo Tanaka¹, and Toshihiro Higuchi¹
¹Neurosurgery, Meiji University of Integrated Medicine, Nantan-shi, Kyoto, Japan, ²Medical Informatics, Meiji University of Integrated Medicine, Kyoto, Japan, ³Biofunctional Imaging, Immunology Frontier Research Center, Osaka University, Osaka, Japan, ⁴Research&Collaboraton, Siemens Japan K.K., Tokyo, Japan

Introduction Typically, functional magnetic resonance imaging (fMRI) studies of acupuncture have been performed using block designs and analyzed using a general linear model (GLM). However, recent studies have questioned the equivalence of stimulations with sensations in block-design acupuncture experiments [1-2]. Furthermore, a previous study showed that prolonging of the needling sensation introduced by acupuncture needling could occur [3]. Once, we reported that acupuncture stimulation induced specific activity that was stronger than activity after the other tactical stimulations. [4-5]. Recently, multi-band (MB) echo planar imaging (EPI) can accelerate the acquisition's temporal resolution to excite the multi slice simultaneously is a popular acquisition for fMRI. Therefore, in this study, we examined the signal change with high temporal resolution in brain activity caused by acupuncture stimulation using MB-EPI and deconvolution analysis.

Methods Twenty-four healthy right-handed subjects (men, 16; women, 8; age range, 18–33 years) were divided into 2 groups. One group (N = 12; 8 men and 4 women) received real acupuncture stimulation with manual manipulation; the other group (N = 12; 8 men and 4 women), which was considered as the control, received tactile stimulation with sham acupuncture (noninsertive) stimulation and scrubbing stimulation. Acupuncture stimulation was applied by bidirectional needle rotation to approximately 180° with even motion at a frequency of 1 Hz. Tactile stimulation consisted of 2 types: tapping the skin at the LI4 with a size 5.88 von Frey monofilament (sham acupuncture stimulation) and scrubbing the skin on the palm using a sponge at 4 Hz.

All fMRI runs consisted of block designs with five 15-s stimulation blocks (on) interspersed between one 30-s and five 45-s rest blocks (off). All experiments were performed using a SIEMENS 3.0-T Trio MRI system with a 32 channel head array coil. The subjects underwent MB gradient echo type-EPI (MB GRE-EPI) with the following parameters: thickness, 3.5 mm; matrix, 64 × 64; field of view (FOV), 22.4 × 22.4 cm²; repetition time (TR), 1000 ms; echo time (TE), 30 ms, flip angles, 60°; MB-factor, 2; iPAT factor, 2; 36 axial slices, and 343 time points.

Data analysis was performed using a combination of analysis packages, including Statistical Parametric Mapping 8 (SPM 8) and Analysis of Functional NeuroImages (AFNI) software. The first 13 data points of each dataset were discarded to obtain the stable state. Volume registration, head motion correction, blurring were performed by SPM 8. For statistical analysis, 3dDeconvolve, which is part of the AFNI package, was used to extract the impulse response functions (IRFs) of the fMRI signals on a voxel-wise basis. First, we assumed that 60TRs, which included 15 TR periods for stimulation, were long enough for extracting IRFs. Then, the 31 tent basis functions (¹T–³¹T) covering -4 to 56 TRs (relative to the stimulus onset) were used to estimate the fitting coefficient (beta estimate). To eliminate the variance in each condition of interest across subjects, a random-effects analysis was performed using a 1-sample *t* test at each voxel across subjects based on their individual beta maps (*p* < 0.001, uncorrected) and clusters with threshold size over 10 voxels (428.75ml³). Further, to examine the IRF, a cubic region of interest was defined using a set of voxels in a 4 × 4 × 4-mm³ portion centered in the maximum *t* value for the area of activation cluster within the Brodmann area. Finally, the time courses of the extracted IRFs were tested at each time point across the stimulations. A one-way ANOVA, followed by a Bonferroni correction were performed for statistical comparisons.

Results & Discussion Figure 1 shows the extracted IRFs in the various brain regions. These data were consistent with the IRFs obtained after deconvolution analysis. In real acupuncture, areas of stimulus-induced activation were observed in the secondary somatosensory cortex (SII), insula, anterior cingulate cortex (ACC), thalamus, and supplementary motor area (SMA). Delayed and long-sustained increases of the signal induced by the real acupuncture were observed after stimulation in these areas. Conversely, in sham acupuncture and scrubbing stimulations, areas of stimulus-induced activation were observed in the SI, SII, thalamus and insula. In the SI and SII, scrubbing-induced signal increases during the period of stimulation were significantly larger than that during other periods. Sham acupuncture and scrubbing evoked responses that decreased more rapidly after cessation of the stimuli than those evoked in real acupuncture. Especially, in real acupuncture, significantly delayed and long-sustained increases of BOLD signals were observed in several brain regions related to pain perception than those observed in sham acupuncture and palm scrubbing. We suggest that the delayed and long-sustained signal increases were caused by peripheral nociceptors, flare responses, and processing of the central nervous system.

Conclusion We used MB-EPI sequence and deconvolution with tent basis function for processing the fMRI data for acupuncture stimulation, and we found delayed increasing and delayed decreasing BOLD signal changes in areas related to pain perception. Further, deconvolution analyses with tent functions are considered as useful in the extraction of complicated, associated brain activity that is delayed and sustained for a long period after various stimulations.

Reference

[1] Ho TJ, et al. Am J Chin Med. 2008; 36(1):55-70; [2] Bai L, et al. Hum Brain Mapp. 2009; 30(11):3445-60; [3] Ho TJ, et al. J Altern Complement Med. 2007; 13(1):13-14. [4] Murase T, et al. ISMRM 2012:2146. [5] Murase T, et al ISMRM 2013:2343.

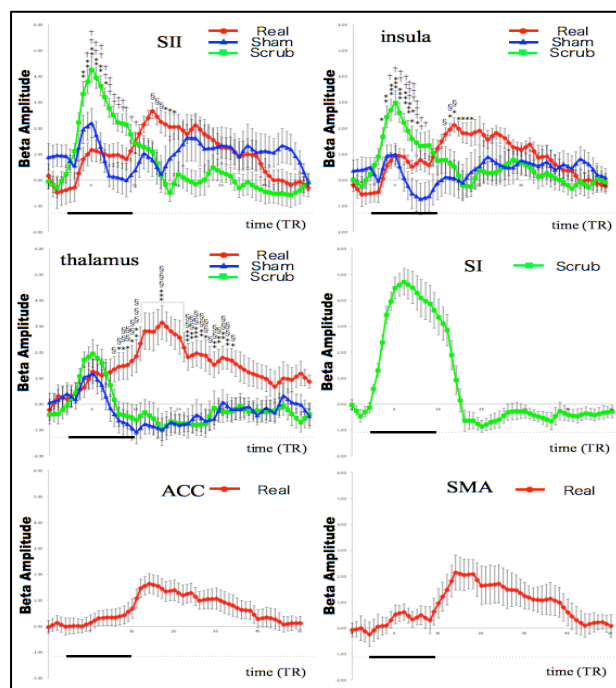


Figure 1 Time-course of the extracted impulse response functions (IRFs; means \pm standard error [SE]) for real acupuncture (red), sham acupuncture (blue), and scrubbing (green) stimulations in the area of the activation cluster. *P* < 0.05: §, †, *, *P* < 0.01: § §, † †, **, *P* < 0.001: § § §, † † †, ***; Real-Sham: †; Real-Scrub: §; Sham-Scrub: *. Black line indicates stimulus duration.